Journal of Magnetism and Magnetic Materials 400 (2016) 311–314

Contents lists available at ScienceDirect

Journal of Magnetism and Magnetic Materials

journal homepage: www.elsevier.com/locate/jmmm

Severe reduction of Ni–Zn ferrites during consolidation by Spark Plasma Sintering (SPS)

Raul Valenzuela [a,*], Thomas Gaudisson [b], Souad Ammar [b]

[a] Instituto de Investigaciones en Materiales, Universidad Nacional Autónoma de México, México D.F. 04510, Mexico
[b] ITODYS, Université Paris-Diderot, PRES Sorbonne Paris Cité, CNRS-UMR-7086, 75205 Paris, France

ARTICLE INFO

Article history:
Received 16 June 2015
Received in revised form
10 July 2015
Accepted 13 July 2015
Available online 14 July 2015

Keywords:
Spark plasma sintering
Nanostructured ferrites
Magnetization in ferrites

ABSTRACT

NiZn ferrites of composition $Zn_{0.7}Ni_{0.3}Fe_2O_4$ were synthesized by the polyol method and subsequently consolidated into fine grain, high density ceramics by means of Spark Plasma Sintering at 600 °C for 10 min, under vacuum and applying a uniaxial pressure of 80 MPa. Their saturation magnetization at room temperature exhibited a value far larger (~71 emu/g) than the value corresponding to the bulk ferrite (~50 emu/g), and their Curie point showed also an increase of about 210 K, as compared with the bulk value. These results, together with the presence of a small amount of metallic Ni, are interpreted in terms of a departure of Ni from the spinel phase and an associated reduction of ferric to ferrous cations to compensate for Ni loss.

1. Introduction

In the last years, magnetic nanoparticles (NPs) have attracted a strong interest by their technological applications in fields as varied as biomedicine [1], environmental science [2], and electronic [3], just to mention a few of them. These applications are based on their unusual properties, which are the result of a combination of a high fraction of atoms on their surface, and the changes in magnetic properties associated also with their nanometer scale size.

For many applications in electronics, however, a solid with high density is needed, instead of a powder. In order to retain the unusual magnetic properties, it is desirable to maintain a nanometric range in the grains of the polycrystalline solid. The classic sintering techniques, based on thermal treatments at high temperatures for long times lead to a very rapid grain growth, thereby losing the magnetic properties of very fine grains. A novel technique to consolidate powders made of NPs into high density solids is Spark Plasma Sintering (SPS) [4]. The SPS technique allows the consolidation of high density samples with very short times and significantly reduced sintering temperatures, with improved magnetic properties [5,6]. The SPS method can also be used for in situ solid state reactions [7], not only for the consolidation of powders.

The SPS technique, however, can subject the powdered sample to a very reducing medium, since the sample is located in a graphite mould, pushed by graphite pistons, normally in a vacuum. For some materials, these conditions can induce a reduction in the valency state of some cations, as is the case of certain ferrites, where some cations can be reduced down to the the metallic state. In this work, we present results obtained on the consolidation of NiZn ferrites with initial composition.

$Zn_{0.7}Ni_{0.3}Fe_2O_4$, synthesized as ~8 nm diameter NPs by the polyol method [8]. Upon consolidation, a small amount of metallic Ni was detected, as well as significant changes in the magnetic properties as compared to those of their conventionally made bulk counterparts. These changes are interpreted in terms of a reduction of a small fraction of ferric to ferrous cations to compensate for the departure of Ni cations from the spinel phase.

The aim of this work is to analyze these results and show that this sintering technique is extremely useful, but some care has to be taken into account concerning the reductive character of the process.

2. Experimental techniques

Ni–Zn ferrite NPs were synthesized by means of the polyol method [8,9]. Stoichiometric amounts of the Fe, Ni and Zn acetates were dissolved in diethyleneglycol (DEG) in a reflux vessel. Hydrolysis reaction was favored by water addition in the ratio of 12 mol for each metal mole. The solution was heated up to the boiling point at 6 °C/min under stirring and maintained in reflux

* Corresponding author.
E-mail address: monjaras@unam.mx (R. Valenzuela).

http://dx.doi.org/10.1016/j.jmmm.2015.07.044
0304-8853/

for 2 h. The suspension was then cooled down to room temperature with continued stirring. The powder precipitate was separated from the suspension by centrifugation, and washed three times with ethanol to remove traces of any organic residue. The solid was then left to dry overnight at 80 °C.

NiZn ferrite NPs were consolidated by SPS. In practice, the starting material (usually a powder) is compressed in a graphite die between two graphite pistons [4], High intensity electric pulses are applied to the die to increase the temperature. The reaction chamber is kept in vacuum, or in a controlled atmosphere. The electric current flows through the die, and also through the sample if it is a conductor. Recent results show that the atom diffusion during the whole process in significantly enhanced by the electric current; even in the case that the sample is a non-conducting material, the applied electric field can promote diffusion [10]. This explains the extremely short sintering times and very low sintering temperatures observed in these processes.

A DR Sintering 515 SPS facility was used (CNRS-Thiais, France). A typical process includes a heating from room temperature up to 280 °C in 10 min (rate ~26 °C/min), a 10 min plateau to eliminate any organic remains in the sample, then a heating up to 600 °C in 10 min (rate ~32 °C/min), and a sintering at this temperature for 10 min, followed finally by a cooling at a rate ~50 °C/min (see Fig.1).

Crystal structures were determined with a Siemens D-5000 diffractometer with CoKα radiation ($\lambda = 1.7930$ Å). Magnetization measurements were carried out in a LDJ 9600 VSM magnetometer with a maximum applied field of 10 kOe, in the 300–500 K temperature.

3. Experimental results and discussion

The X-ray diffraction pattern (XRD) of polyol synthesi-zed NPs exhibited the characteristic diffraction peaks of the spinel structure, Fig. 2(a).

The calculated unit cell parameter for NPs was $a_{NPs} = 8.417 \pm 0.009$, which is close to the cell parameter in the bulk ferrite [11]. TEM observations, Fig. 3, of these NPs showed that their shape was almost spherical, with dimensions in the 6–10 nm range.

The XRD pattern of the ceramic resulting from SPS consolidation of these NPs is almost consisting with that of NPs. Indeed it matches very well with that of the spinel structure (Fig. 2(b)).

The unit cell parameter of the spinel phase was found to be somewhat smaller than that measured previously: $a_{SPS} = 8.406 \pm 0.002$. Note the linewidths are extremely narrow as compared with the XRD peaks of the NPs pattern. This is a normal result, as long as the consolidation process involves grain growth

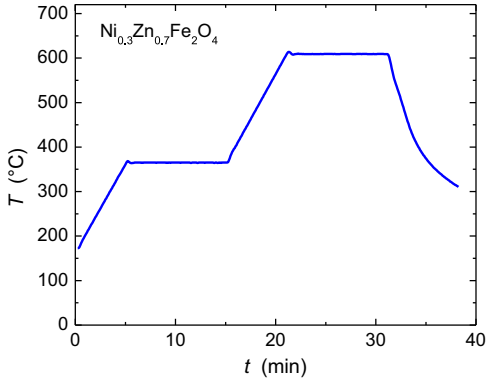

Fig. 1. Time-temperature profile of the SPS process.

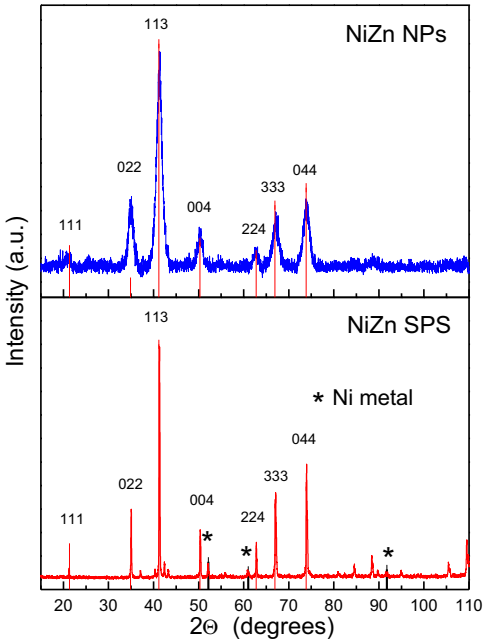

Fig. 2. X-ray diffraction patterns of the NPs (up), and the consolidated ceramic (below).

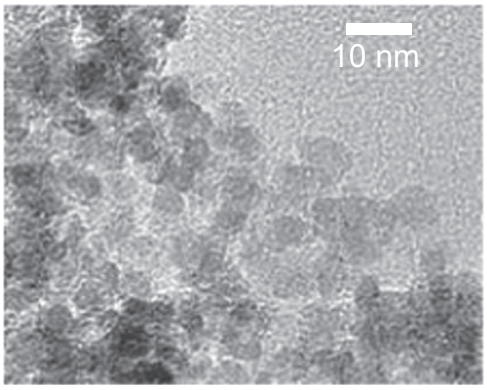

Fig. 3. HRTEM micrography of NPs as obtained.

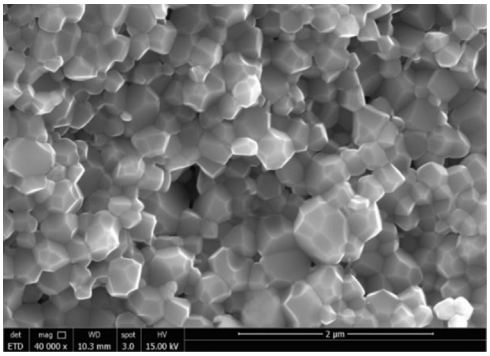

Fig. 4. SEM micrography of consolidated ceramic.

and the formation of a polycrystalline structure, where the NPs free surfaces have been changed to grain boundaries, as can be observed on Fig. 4. The effective size of crystals increases considerably. The obtained solid had a density 4.88 g/cm^3 (~92% of the theoretical density for this composition).

By looking into the detail in the XRD from the SPS consolidated sample, there are some peaks additional to the spinel structure. These peaks have been identified as belonging to metallic nickel.

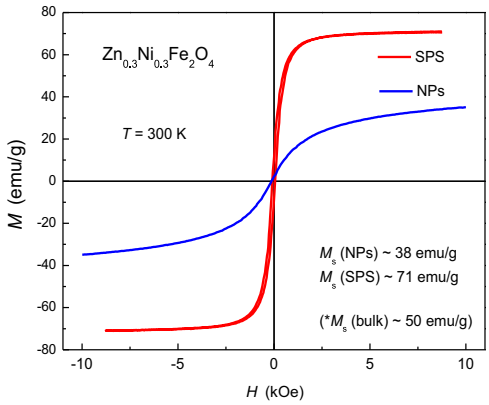

Fig. 5. Hysteresis loops of NPs and consolidated ceramic at room temperature. The values of saturation magnetization are given, including the value for bulk ferrite.

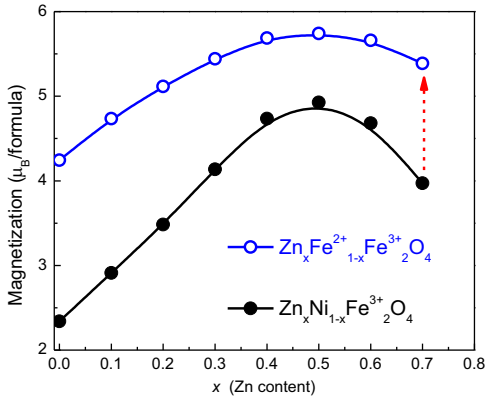

Fig. 6. Behavior of the magnetic moment per formula for ZnNi and ZnFe ferrites, at low temperatures (adapted from [12,13]). The arrow shows the expected change in magnetization with loss of Ni and introduction of Fe^{2+}.

The magnetic hysteresis loops of both samples (NPs and SPS), taken at room temperature, is presented in Fig. 5, showing remarkable differences. The loops belonging to NPs exhibits a superparamagnetic behavior, lacking coercive field and remanent magnetization. The sample prepared by SPS, in contrast, shows a behavior typical of a magnetically ordered material with low anisotropy, with "shoulders" tending to a rectangular shape. The superparamagnetic behavior is explained by the fact that these NPs possess a low magnetocrystalline anisotropy, and with such small dimensions, the thermal energy becomes comparable, or even larger than the total anisotropy for each NP.

A ZFC-FC experiment (Fig. 6) confirms that the blocking temperature is about 70 K.

In Fig. 5 there is a fact, however, which requires an explanation more elaborated: the saturation magnetization of these two hysteresis loops exhibited very different values. For the NPs sample, $M_s \sim 38$ emu/g, while for the SPS sample, M_s attains more than 70 emu/g. Since $M_s \sim 50$ emu/g for the bulk [11], the magnetization value shown by the NPs seems reasonable taking into account that it is a superparamagnetic phase, relatively far from the saturation state. In contrast, the value for the SPS-consolidated sample is some 20 emu/g larger than the bulk. Such difference points to an important change in the ferrite structure, associated with the SPS process.

The presence of metallic nickel, Ni^0, in the XRD pattern (Fig. 2 (b)) can give some insight on the changes during the SPS process. By taking roughly the relative Ni^0 content (in at%) as the intensity ratio between the main diffraction peaks [(311) for the ferrite and (111) for the nickel [ICDD no. 00-004-0850]], the result is ~6 at%.

If the total Ni content in the ferrite from the formula $Ni_{0.3}Zn_{0.7}Fe_2O_4$, is calculated, this gives ~4.48 at%. It appears therefore that virtually all the nickel has been reduced and removed from the spinel phase and moved to a second metallic phase.

In order to compensate for this loss of divalent cation, and maintain the electric neutrality in the spinel phase, it can be assumed that an equivalent amount of ferric cations are reduced to the ferrous state, leading to the new composition in the spinel phase, $Zn_{0.7}Fe^{2+}_{0.3}Fe^{3+}_2O_4$. If we further assume that this new spinel phase possesses the cation distribution of the bulk, i.e., zinc cations on the tetrahedral sites, ferrous ions on the octahedral sites, and ferric cations on both, we can represent the ferrite as: $\left(Zn_{0.7}Fe^{3+}_{0.3}\right)\left[Fe^{2+}_{0.3},\ Fe^{3+}_{1.7}\right]$. The overall stoichio-metry of the spinel phase is maintained, as far as the total divalent cations are $0.7Zn+0.3Fe^{2+}$. There are two trivalent cations Fe^{3+}, for every four oxygens, as shown in the formula $Zn_{0.7}Fe^{2+}_{0.3}Fe^{3+}_2O_4$.

The substitution of Ni^{2+} by Fe^{2+} on octahedral sites leads to a significant increase in magnetization, as the magnetic moment of Fe^{2+} is larger (4.2 μB) than that of Ni^{2+} (2.3 μB). A plot of magnetic moment as a function of the Zn content, *x*, for these ferrite solid solutions [12,13], shows that the Fe^{2+} solid solution exhibits a larger magnetic moment by formula, see Fig. 6.

We also estimated the Curie transition of the SPS sample, T_C, by measuring the hysteresis loops as a function of temperature (not presented here). T_C is roughly the temperature where the hysteresis loop becomes a straight line with a small slope, which is the indication of a paramagnetic phase. This temperature is about 533 K, while it is 320 K for the NPs, and 323 for the bulk [14]. This effect in the SPS prepared sample can also be ascribed to the presence of ferrous ions on octahedral sites, as Fe^{2+} (a $3d^4$ ion) can establish a stronger superexchange interaction with Fe^{3+} cations ($3d^5$ ions) on A sites, than Ni^{2+} cations ($3d^8$ ions); half-filled 3d orbitals are more efficient [15] for these interactions. Consistenly, the reported Curie temperature for $Zn_{0.4}Fe_{0.6}Fe_2O_4$ is 624 K [16].

4. Conclusions

These results thus show that the SPS method is very convenient to sinterize oxides. It is especially efficient when combined with oxide NPs, to perform a consolidation at very low temperatures and extremely short sintering times, as compared with the classic, solid state methods. An additional advantage is that final grain size in the resulting polycrystalline solid can be maintained within in the 200 nm range. However, since it is carried out in a vacuum, and the powder is pressed in a graphite mould, it can be subjected to strong reducing conditions. In our case, this reduction in NiZn ferrites led to the partial reduction of Fe^{3+} to Fe^{2+} to compensate for the extraction of Ni^{2+} to metallic Ni^0.

Acknowledgments

Authors acknowledge the contribution from Dr. Manuel Bañobre (International Nanotechnology Laboratory, Braga, Portugal) and Prof. José Rivas Rey (Universidad de Santiago de Compostela, Spain), for electron microscopy and useful discussions, as well as Y. Flores for assistance with experiments.

References

[1] H.M. Joshi, J. Nanopart. Res. 15 (2012) 1.
[2] S.C.N. Tang, I.M.C. Lo, Water Res. 47 (2013) 2613.
[3] D. Sellmyer, R. Skomski, Advanced Magnetic Nanostructures, Springer-Verlag,

New York, 1959.
[4] R. Orru, R. Lichen, A.M. Locci, G. Cao, Mater. Sci. Eng. R 63 (2009) 127.
[5] N. Millot, S. Le Gallet, D. Aymes, F. Bernard, Y. Grin, J. Eur. Ceram. Soc. 27 (2007) 921.
[6] S. Imine, F. Schenstein, S. Mercone, M. Zaghirioui, N. Bettahar, M. Jouini, J. Eur. Ceram. Soc. 31 (2007) 2943.
[7] S. Imine, F. Schenstein, W. Jiang, Int. J. Refract. Met. 39 (2013) 103.
[8] S. Chkoundali, S. Ammar, N. Jouini, F. Fievet, M. Richard, P. Molinie, F. Villain, J. M. Greneche, J. Phys. Condens. Matter 16 (2004) 4357.
[9] H. Basti, L. Ben Tahar, L.S. Smiri, F. Herbst, M.J. Vaulay, F. Chau, S. Ammar, S. Bendervous, J. Colloid Interface Sci. 341 (2) (2010) 248.
[10] Z.A. Munir, U. Anselmi-Tamburini, M. Ohyanagi, J. Mater. Sci. 41 (2006) 763.
[11] R. Valenzuela, Magnetic Ceramics, Cambridge University Press, Cambridge, UK, 2005.
[12] E.W. Gorter, Philips Res. Rep. 9 (1954) 295.
[13] C. Guillaud, M. Sage, Comptes Rendus de l'Académie des Sci. 232 (1951) 944.
[14] A. Globus, H. Pascard, V. Cagan, J. Phys. C1-38 (1977) C1-163-8.
[15] J. Kanamori, J. Phys. Chem. Solids 10 (1959) 87.
[16] C.M. Srivastava, S.N. Shringi, R.G. Srivastava, N.G. Nanadikar, Phys. Rev. B 14 (1976) 2032.